ECCM 2010
IV European Conference on Computational Mechanics
Palais des Congrès, Paris, France, May 16-21, 2010

Bifurcations of an elastic model with nonsmooth material law

Z. Gáspár[1], T. Tarnai[1], K. Hincz[1]

[1] *Budapest University of Technology and Economics, Hungary, {gaspar@ep-mech.me.bme.hu, tarnai@ep-mech.me.bme.hu, hinczkrisztian@yahoo.com}*

Abstract – How must 5 equal discs of given radius *r* be arranged on the unit circle so that the area of the intersection of the unit circle and the union of the 5 discs will be a maximum; and how does the solution change if *r* varies from the maximum packing radius to the minimum covering radius? In this paper, a mechanical model is introduced to analyse this mathematical problem. A generalized tensegrity structure is associated to a maximum area configuration of the 5 discs, and by using catastrophe theory, it is pointed out that the "equilibrium paths" have bifurcations, that is, at certain values of *r*, the type of the tensegrity structure and so the type of the disc configuration changes.

1. Introduction

One of the well-known problems in discrete geometry is the following [2]: How must *n* equal circles be packed in the unit circle without overlapping so that the radius of the circles will be as large as possible? This *packing* problem has a dual counterpart in *covering*: How must the unit circle be covered by *n* equal circles without interstices so that the radius of the circles will be as small as possible? For a given *n*, let $r_{\max}$ and $R_{\min}$ denote the maximum radius in the packing problem and the minimum radius in the covering problem, respectively. For circles with radius *r* such that $r_{\max} \le r \le R_{\min}$, recently, Connelly [3] posed a problem *intermediate* between these two: How must the centres of *n* equal discs of given radius *r* be distributed in the unit circle so that, in the unit circle, the area covered by the discs will be a maximum? This *intermediate* problem is the topic of the present paper. It should be noted that earlier Fejes Tóth [5] raised and Fowler and Tarnai [6] analysed numerically a similar intermediate problem on the sphere.

Connelly [3] considered the case of $n = 5$ as an example (see Figure 1), and wanted to know that, with a continuous increase in *r*, how the disc configuration changes in the transition from the maximum packing to the minimum covering.

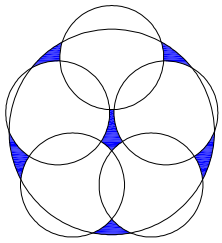

Figure 1: Arrangement of 5 equal circles in a unit circle, the uncovered area is in blue

If *r* is close to the maximum packing radius then the discs have only double overlaps, like in Figure 1. In this case, the maximum area can be determined with a formula of Csikós [4]. Connelly [3] worked out a stress interpretation of Csikós's formula, and showed how a tensegrity structure can be associated to the maximum area configuration. However, if *r* is close to the minimum covering radius then the discs can have some triple overlaps for which, though Csikós's formula is still valid, it is not known how to construct a mechanical model to represent the maximum area configuration.

In this paper, we will show that, in the case of triple overlaps, the equivalent mechanical model of the maximum area configuration of discs is a generalized tensegrity structure which, additionally to struts and cables, contains also triangular elements (known as in-plane loaded plate elements in the finite element techniques). In the numerical investigation, stability problems of the configuration were

found for certain values of r. If r is plotted against properly selected active variables then space curves analogous to equilibrium paths are obtained where, at certain points, bifurcation phenomena are detected. Catastrophe theory will be used to analyse these bifurcations, properties of some of which, however, are beyond the elementary catastrophe theory [7]. At general points of the "equilibrium paths", the numerical calculation was executed with the method of dynamic relaxation, while to determine the bifurcation points, iteration using the tangent stiffness matrix of the structure was applied. The different phenomena and properties will be shown through the example of the intermediate problem of 5 discs.

2. Packing of 5 equal circles

As shown first by Graham [8], the largest radius of circles which can be arranged in the unit circle without overlapping is

$$r_{\max} = \frac{\sin(\pi/5)}{1+\sin(\pi/5)} = 0.3701919083.$$

The arrangement has D_{5h} symmetry. The (local) optimum of the arrangement can be checked by a bar-and-joint model (see Figure 2). The joints of the structure are the centres of the circles; two joints are connected by a bar if the corresponding circles touch each other. Each joint laying on the circle with radius $1-r$ is supported by a roller in the radial direction. If the arrangement is optimal, then the structure can be in a state of self-stress where there are no bars in tension [9].

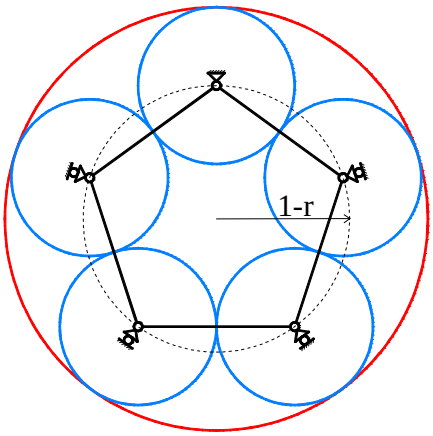

Figure 2: Maximum packing of 5 equal circles in the unit circle, and its mechanical model

3. Covering by 5 circles

One might think that the optimal covering has also D_{5h} symmetry, where the radius is

$$R = \frac{1}{2\cos(\pi/5)} = 0,6180339890\,.$$

The optimal covering can be checked by another model based on a bipartite graph, where the vertices of the first kind are the centres of the circles and the vertices of the second kind are the points of the perimeters of the circles in which the unit circle is only just covered. (In Figure 3, the vertices of the first kind are marked by small circles but the vertices of the second kind have no special mark.)

The centre of the unit circle is covered by 5 circles. In such a case this second kind vertex must be tripled, and suitable bars must be doubled while three bars will meet at each vertex (see Figure 4 left). If a covering is optimal, then the structure can be in a state of self-stress where there are no bars in compression [10]. Since in this case some bars are in compression, they ought to be dropped, and the whole structure can be cooled while we arrive to the optimal state which is shown in the right side of Figure 4. As proved by Bezdek [1], the smallest radius when 5 circles can cover the unit circle is $R_{\min} = 0.6093828641$. This structure can be in a state of self-stress with all bars in tension.

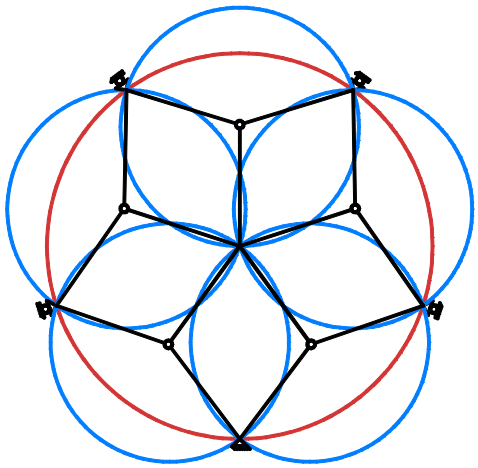

Figure 3: Covering the unit circle by 5 equal circles in D_{5h} symmetry, and its mechanical model

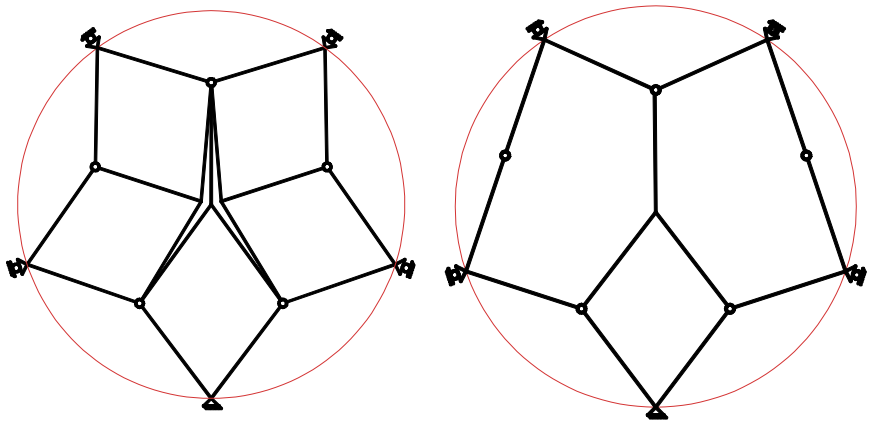

Figure 4: Model with a tripled vertex (left side) and the model of the optimal covering (right side)

4. Transition from packing to covering

If r is only a little larger than the maximum packing radius $\left(r_{\max}\right)$ then the discs have double overlaps (pairwise intersections). In such a case, the motion of the discs can be described as a function of a parameter, and the derivative of the area with respect to the motion parameter can be expressed with a formula of Csikós [4]. The condition, that the derivative is equal to zero, determines the maximum area configuration of the discs. Connelly has provided a stress interpretation of Csikós's formula, and shown how a tensegrity framework can be associated to the maximum area configuration. However, if r is close to the minimum covering radius, then the discs have some triple overlaps for which it is not known how to set up an equivalent mechanical model to obtain the solution to the mathematical problem.

In this paper, we introduce cables to model the overlaps of a circle and the unit circle, struts to model the overlaps of two circles, and triangular elements to model the triple overlaps of the circles (see Figure 5). Since the types of the symmetry are different for the optimal packing and covering, there must be some stability phenomena while r increases from $r_{\max}$ to $R_{\min}$.

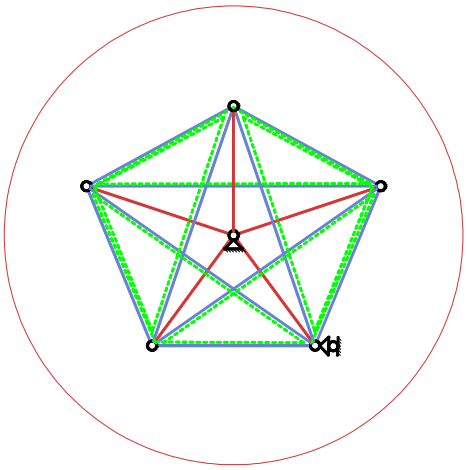

Figure 5: The model contains 5 cables (red), 10 struts (blue) and 5 triangular elements (green)

4.1. Material laws

The material laws are nonsmooth.

Cables

If a circle intersects the unit circle, the corresponding cable becomes active, and a tensional force (S) arises in it. The magnitude of this force is

$$S = \frac{dA_1}{dL} = \begin{cases} 0 & \text{if } L \le 1 - r \\ \sqrt{4L^2 - \left(1 + L^2 - r^2\right)} / L & \text{if } L > 1 - r \end{cases}$$

which is equal to the length of the chord between the two points of intersection (see Figure 6).

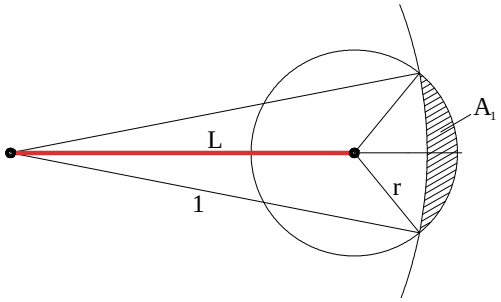

Figure 6: Intersection of a small circle with the unit circle

Struts

If a circle intersects the unit circle, the corresponding strut becomes active, and a compression force (S) arises in it. The magnitude of this force is

$$S = \frac{dA_2}{dL} = \begin{cases} -\sqrt{4r^2 - L^2} & \text{if } L < 2r \\ 0 & \text{if } L \ge 2r \end{cases},$$

which is equal to the length of the chord between the two points of intersection (see Figure 7).

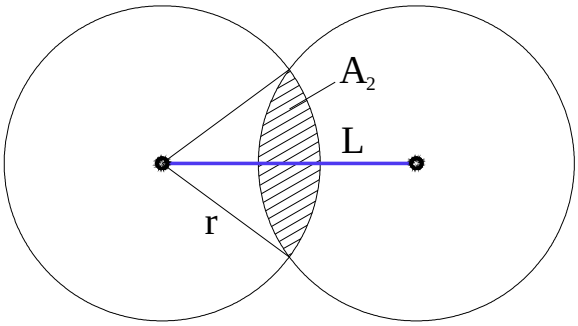

Figure 7: Intersection of two small circles

Triangular elements

If three circles have an area in common, the corresponding triangular element becomes active, and tensional forces $(Q_i, i=1,2,3)$ might arise in its edges. Magnitudes of these forces are (see Figure 8):

$$Q_i = \frac{\partial A_3(L_1, L_2, L_3)}{\partial L_i}.$$

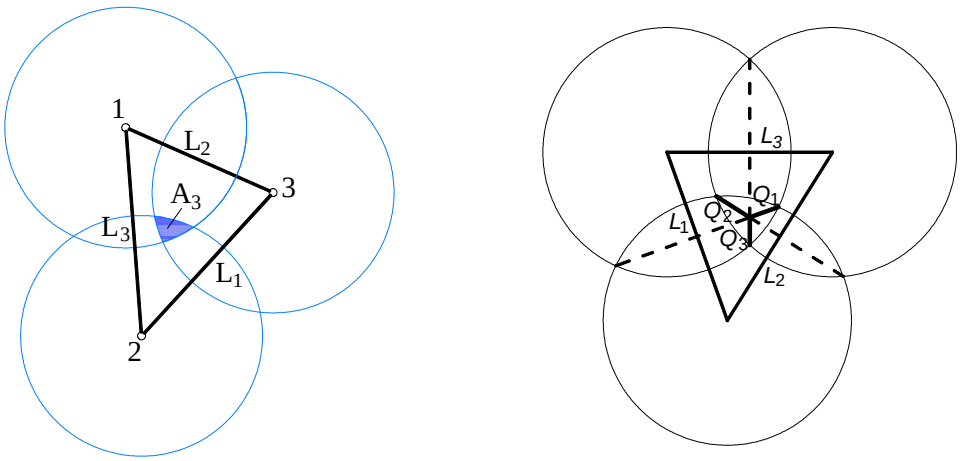

Figure 8: The common area of three circles (left) and the geometrical explanation of the forces (right)

The geometrical explanation of the edge forces is the following: we have considered the compression force in a strut as the length of the appropriate chord, but only the length of the appropriate edge of the Voronoi cell will appear in it. So the magnitude of the edge (tension) forces is the difference of the two lengths.

Angles of the triangle are (we use a cyclic order among the subscripts):

$$\beta_i = \arccos \frac{L_{i-1}^2 + L_{i+1}^2 - L_i^2}{2L_{i-1}L_{i+1}}.$$

Radius of the circle drawn through the vertices of the triangle (for any *i*):

$$R = \frac{L_i}{2\sin\beta_i}.$$

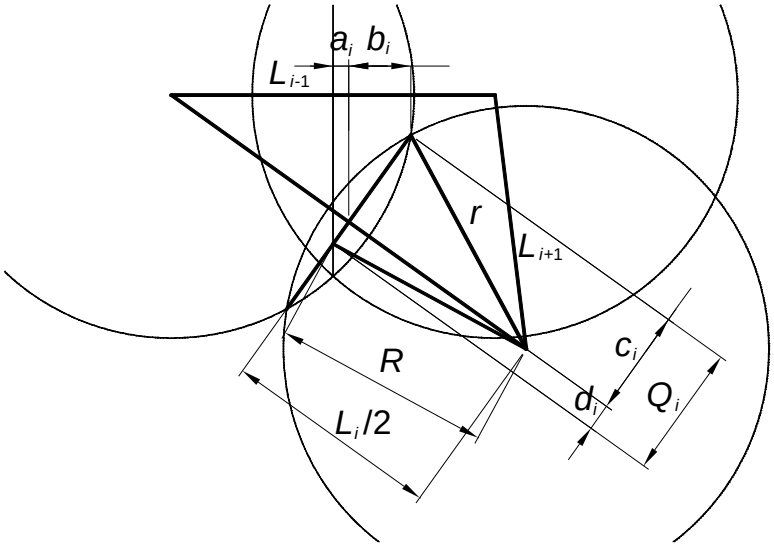

Figure 9: Explanation of the variables

If $R > r$ then the triangular element is passive (every edge force is zero). If $R < r$, then the auxiliary variables shown in Figure 9 are:

$$a_i = \frac{L_i^2 - L_{i-1}^2 - L_{i+1}^2}{4L_{i-1}}, \qquad c_i = \sqrt{r^2 - L_i^2/4},$$

$$b_i = c_i \sin\beta_{i+1}, \qquad d_i = \sqrt{R^2 - L_i^2/4}.$$

The edge forces:

$$Q_i = \begin{cases} 2c_i & \text{if } 0 < a_i - b_i \\ c_i + d_i & \text{if } a_i - b_i < 0 < a_i \\ c_i - d_i & \text{if } a_i < 0 < a_i + b_i \\ 0 & \text{if } a_i + b_i < 0 \end{cases}.$$

4.2. Solution by dynamic relaxation

Using the model shown in Figure 5 and the constitutive equations given in Subsection 4.1 with the help of the dynamic relaxation, one can compute an equilibrium position for any given $r \in (r_{\max}, R_{\min})$. The radius is increased in small steps in this interval. For every r we start the iteration with the final coordinates of the arrangement belonging to the previous value of r. Figure 10 shows the coverage of the unit circle as the function of r.

Different types of the shapes are shown with different colours, one example for each type is shown in Figure 11.

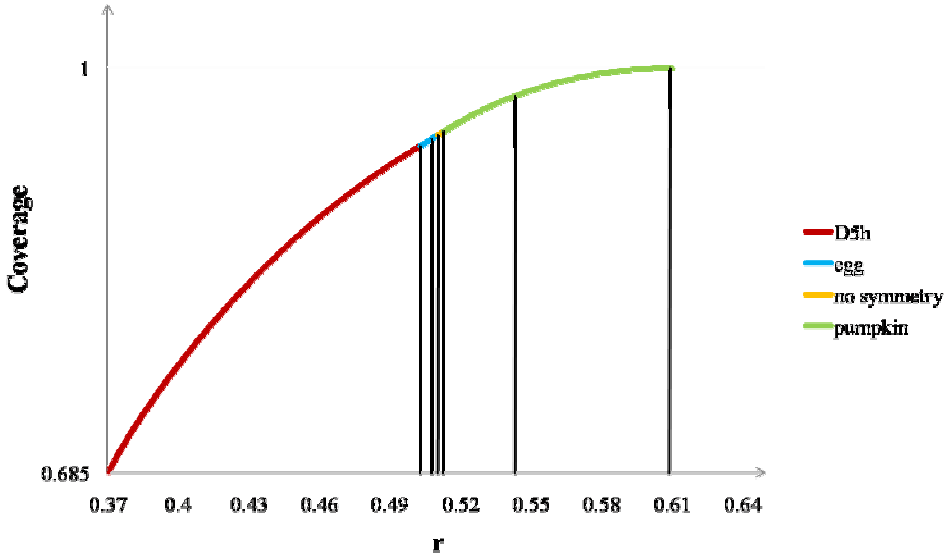

Figure 10: Coverage as function of the radius

a) b)

c) d)

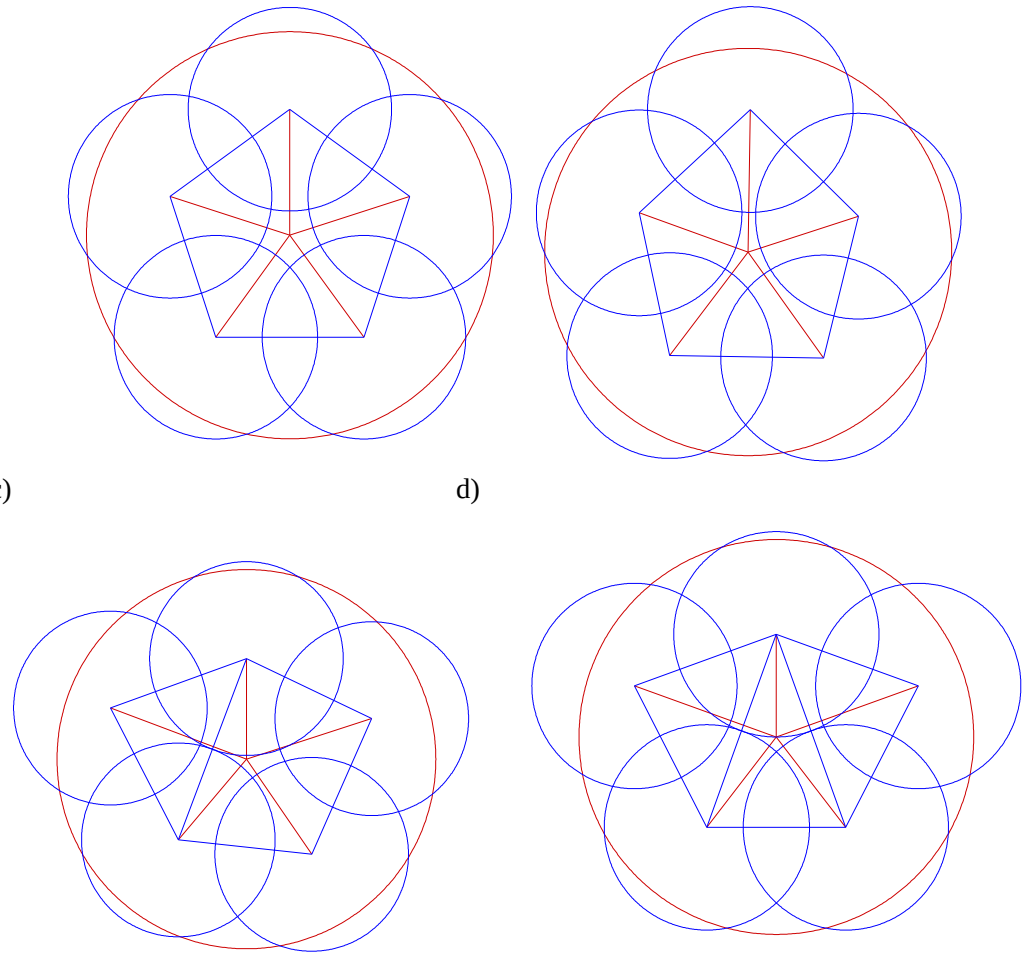

Figure 11: Different types of shape: (a) D_{5h} r=0.500, (b) egg r=0.505, (c) no symmetry r=0.511, (d) pumpkin r=0.520

Figure 12 shows that the number of the iteration steps increases very strongly when the type of the shape changes. One might think that the dynamic relaxation converges to the optimal arrangement for every fixed radius, but the borders between the shape types may change a little if we start with a large value of *r*, and we decrease it step by step using the same values as earlier. Of course we can use smaller steps, but this method is suitable neither to compute the exact value of the borders nor to find every equilibrium path (so to determine the types of the bifurcation points). To answer these questions, we deal with the stiffness matrix of the structure.

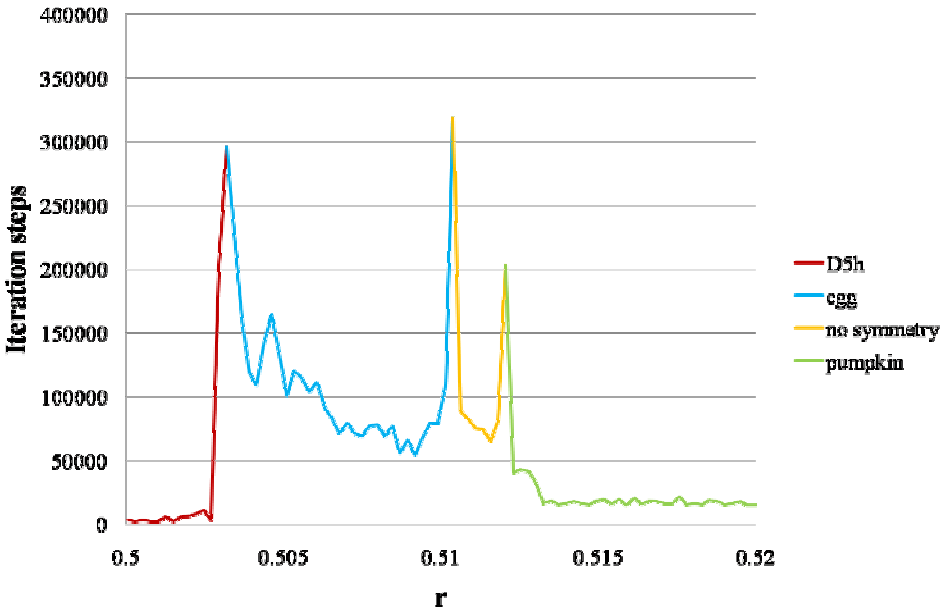

Figure 12: Number of the iteration steps as the function of the radius

4.3. Stiffness matrices

The stiffness (H) of the cable is

$$H=\frac{dS}{dL_S}=\begin{cases}0 & \text{if } S=0\\ \dfrac{1}{L_S}\left(\dfrac{2\left(1-L_S^2+r^2\right)}{S}-S\right) & \text{if } S>0\end{cases},$$

and that of a strut

$$H=\frac{dS}{dL_s}=\begin{cases}\sqrt{4\left(r/S\right)^2+1} & \text{if } S<0\\ 0 & \text{if } S=0\end{cases},$$

where L_s is the length belonging to the force S, i. e. for a cable

$$L_s=\begin{cases}L_r & \text{if } S=0\\ \sqrt{1+r^2-S^2/2-\sqrt{4r^2-S^2-r^2S^2+S^4/4}} & \text{if } S>0\end{cases}$$

and for a strut

$$L_s=\begin{cases}\sqrt{4r^2-S^2} & \text{if } S<0\\ L_r & \text{if } S=0\end{cases}.$$

The stiffness matrix of these elements has the following structure

$$\mathbf{K}=\begin{bmatrix}\mathbf{K}_0 & -\mathbf{K}_0\\ -\mathbf{K}_0 & \mathbf{K}_0\end{bmatrix},$$

where

$$\mathbf{K}_0 = \mathbf{e}\mathbf{e}^T\left(H - \frac{S}{L_r}\right) + \mathbf{E}\frac{S}{L_r}.$$

Stiffness of a triangle gives the relationship between an infinitesimal change in the edge forces and that in the edge lengths:

$$\begin{bmatrix} dQ_1 \\ dQ_2 \\ dQ_3 \end{bmatrix} = \mathbf{H}\begin{bmatrix} dL_1 \\ dL_2 \\ dL_3 \end{bmatrix}.$$

The elements of matrix **H** are:

$$H_{ij} = \frac{\partial Q_i}{\partial L_j} = \begin{cases} 2\dfrac{\partial c_i}{\partial L_j} & \text{if } 0 < a_i - b_i \\ \dfrac{\partial c_i}{\partial L_j} + \dfrac{\partial d_i}{\partial L_j} & \text{if } a_i - b_i < 0 < a_i \\ \dfrac{\partial c_i}{\partial L_{j\,i}} - \dfrac{\partial d_i}{\partial L_j} & \text{if } a_i < 0 < a_i + b_i \\ 0 & \text{if } a_i + b_i < 0 \end{cases},$$

where (δ_{ij} is the Kronecker symbol)

$$\frac{\partial c_i}{\partial L_j} = \frac{-\delta_{ij} L_i}{4\sqrt{r^2 - L_i^2/4}},$$

$$\frac{\partial d_i}{\partial L_j} = \frac{R\dfrac{\partial R}{\partial L_j} - \delta_{ij}\dfrac{L_i}{4}}{\sqrt{R^2 - L_i^2/4}},$$

$$\frac{\partial R}{\partial L_j} = \frac{L_{j-1}L_{j+1}\left(L_j^4 - \left(L_{j-1}^2 - L_{j+1}^2\right)^2\right)}{\left(2L_j^2L_j^2 + 2L_j^2L_j^2 + 2L_j^2 - L_j^4 - L_j^4 - L_j^4\right)^{3/2}}.)$$

The primary stiffness matrix $\left(\mathbf{K}'\right)$ of a triangular element provides the relationship between the nodal displacement increments and the nodal load increments equilibrating the edge force increments arising from the nodal displacement increments:

$$\begin{bmatrix} dq_{1x} \\ dq_{1y} \\ dq_{2x} \\ dq_{2y} \\ dq_{3x} \\ dq_{3y} \end{bmatrix} = \begin{bmatrix} & -\mathbf{e}_2 & \mathbf{e}_3 \\ \mathbf{e}_1 & & -\mathbf{e}_3 \\ -\mathbf{e}_1 & \mathbf{e}_2 & \end{bmatrix}\mathbf{H}\begin{bmatrix} & \mathbf{e}_1^T & -\mathbf{e}_1^T \\ -\mathbf{e}_2^T & & \mathbf{e}_2^T \\ \mathbf{e}_3^T & -\mathbf{e}_3^T & \end{bmatrix}\begin{bmatrix} dv_{1x} \\ dv_{1y} \\ dv_{2x} \\ dv_{2y} \\ dv_{3x} \\ dv_{3y} \end{bmatrix} = \mathbf{K}'d\mathbf{v},$$

that is, a submatrix of $\mathbf{K}'$ is

$$\mathbf{K}'_{ij} = \sum_{\alpha=1}^{2}\sum_{\beta=1}^{2}(-1)^{i+j+\alpha+\beta}\,\mathbf{e}_{i+\alpha}H_{i+\alpha,j+\beta}\mathbf{e}_{j+\beta}^T,$$

where $\mathbf{e}_i$ is the unit vector of the *i*th edge, and, among the subscripts, the above-mentioned cyclic order is valid.

The secondary (supplementary) stiffness matrix of the triangular element contains the effect of the change in the position of the edge forces developed earlier. A submatrix of the main diagonal of the supplementary stiffness matrix of the *i*th edge is

$$\mathbf{K}_i^0 = \frac{Q_i}{L_i}\left(\mathbf{E} - \mathbf{e}_i\mathbf{e}_i^T\right),$$

so, the supplementary stiffness matrix of a triangular element is

$$\mathbf{K}'' = \begin{bmatrix} \mathbf{K}_2^0 + \mathbf{K}_3^0 & -\mathbf{K}_3^0 & -\mathbf{K}_2^0 \\ -\mathbf{K}_3^0 & \mathbf{K}_1^0 + \mathbf{K}_3^0 & -\mathbf{K}_1^0 \\ -\mathbf{K}_2^0 & -\mathbf{K}_1^0 & \mathbf{K}_1^0 + \mathbf{K}_2^0 \end{bmatrix}.$$

The complete (tangent) stiffness matrix of a triangular element is the sum of the two stiffness matrices:

$$\mathbf{K} = \mathbf{K}' + \mathbf{K}''.$$

4.4. Equilibrium paths

The optimal arrangement has a D_{5h} symmetry if $r < r_1 = 0.502995$. At r_1 the stiffness matrix becomes singular. If we force the structure to remain symmetric with respect to the vertical axis then we have the eigenvector of the stiffness matrix shown on the right side of Figure 13. The generalized coordinate u shows the magnitude of this displacement. If $u > 0$ the circles form an egg shape, if $u < 0$ we have a pumpkin shape.

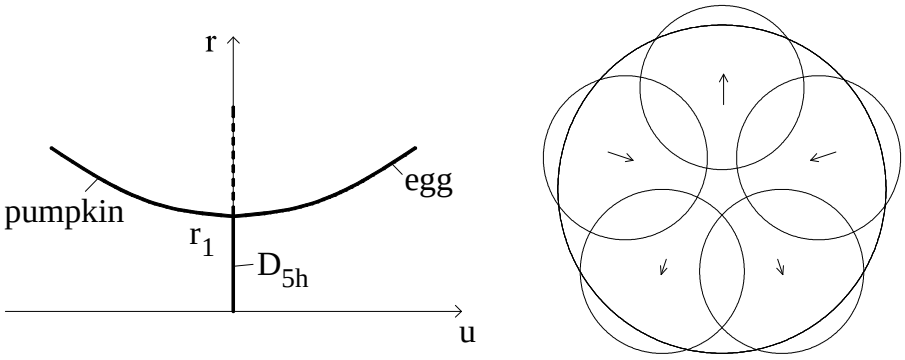

Figure 13: Bifurcation at *r*=0.502995

One might think that this is a stable symmetric bifurcation (standard cusp catastrophe), but this is not true because the co-rank of the stiffness matrix is two, and the equilibrium paths together have C_{5v} symmetry (see Figure 14).

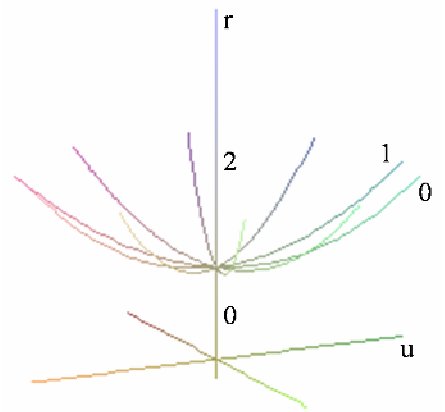

Figure 14: Equilibrium paths at *r*=0.502995, integers show the numbers of the negative eigenvalues

In a suitable cylindrical coordinate system (V,u,φ) the 5-jet of the active part of the potential energy function can be written as

$$V=-\frac{1}{2}\lambda u^2+\frac{1}{4}u^4+\frac{1}{5}u^5\cos 5\varphi,$$

where $\lambda=r-r_1$. This shows that, at the bifurcation point, we have the 12th class of the double cusp catastrophe [7]. If r is a little bit larger than r_1 then egg shapes are stable and the pumpkin shapes are unstable equilibrium positions.

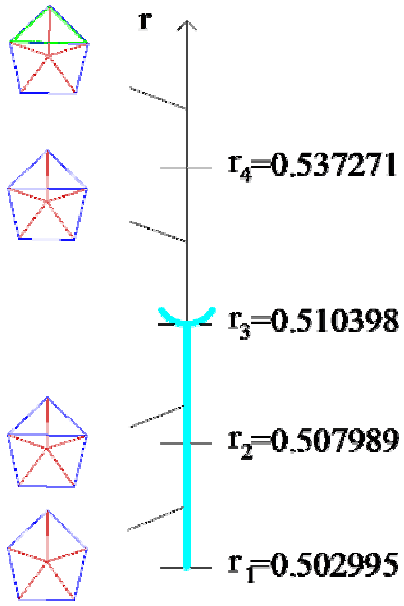

Figure 15: Egg shape equilibrium path

Following the egg shape equilibrium path (see Figure 15) at $r_2=0.507989$ a new strut arises but the path remains stable. There is a stable symmetric point of bifurcation (stable cusp catastrophe) at $r_3=0.510398$. If $r>r_3$ then the egg shape becomes unstable, but the secondary paths are stable. They belong to asymmetric arrangements. Finally, following the egg shape path, an active triangular element appears at r_4=0.537271.

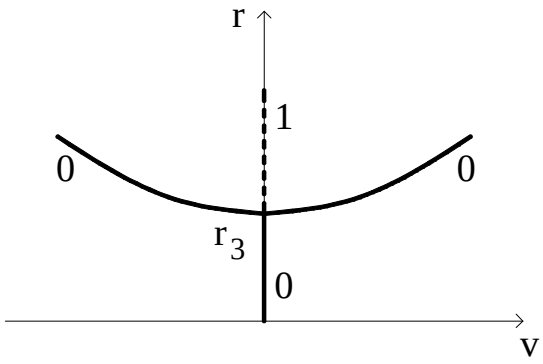

Figure 16: Stable symmetric point of bifurcation at r=0.510398

Similarly, following the pumpkin shape equilibrium path (see Figure 17), at r_5=0.513056 two new strut elements arise. This shows a nonsmooth change in the eigenvalues of the stiffness matrix,

and additionally, the only negative eigenvalue jumps to a positive value. Two active triangular elements arise at r_6=0.543191, and this type of structure is optimal until the covering.

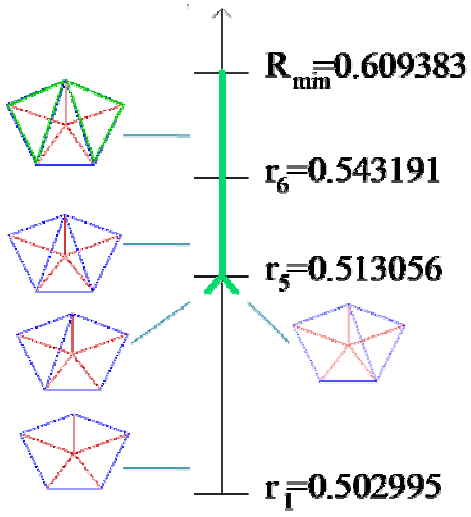

Figure 17: Pumpkin shape equilibrium path

But what happens to the stable equilibrium paths belonging to the asymmetric arrangements? Left part of Figure 18 shows the projection of an egg shape equilibrium path and two neighbouring pumpkin shape equilibrium paths. The asymmetric shape path meets the egg shape paths at r_3 and it connects to the pumpkin shape paths at r_5. At this bifurcation point the potential energy function is not smooth, because in its neighbourhood there are four different topologies of the active elements (and what is more the stiffness of a new element is infinite). If $r > r_5$ then there are seven struts. On the connected asymmetric shape path, one (but different) strut disappears, and on the pumpkin shape path, both of them disappear if $r < r_5$. The connected two asymmetric paths do not form a smooth path.

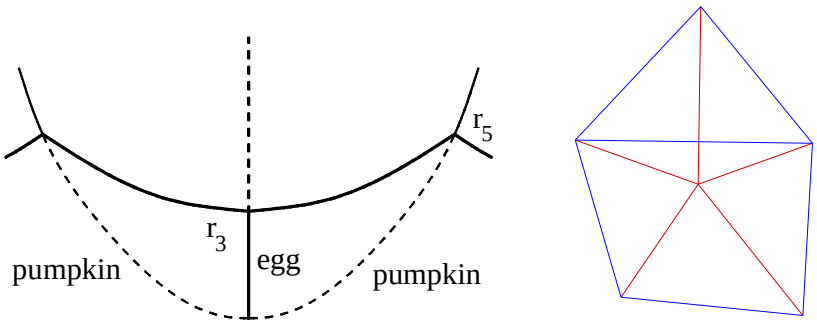

Figure 18: Connections of the asymmetric equilibrium path to the egg shape paths and pumpkin shape paths (left), and the active elements of the asymmetric structure (right)

Figure 19 shows the top view of all the 5 egg, the 5 pumpkin, the 5 asymmetric shape paths (the path of D_{5h} symmetry is parallel with the direction of the projection, so it looks a point). These paths form the very special double cusp catastrophe point, the five standard cusp catastrophe points and the five degenerate bifurcations which do not appear in the elementary catastrophe theory, since the potential energy function is not smooth at these bifurcation points.

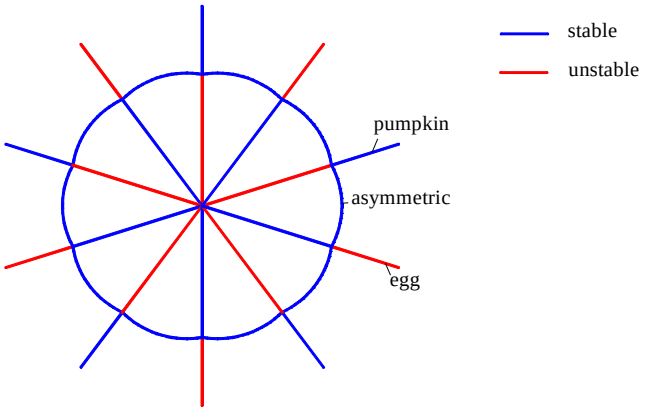

Figure 19: Top view of the equilibrium paths

5. Conclusions

For numerical investigation of problems of packings and coverings with circles, the heating and cooling techniques are mechanically well-established algorithms [9, 10]. In packing and covering problems, an arrangement is locally optimal, if in this position the associated bar-and-joint structure is in equilibrium with a state of self-stress. For investigation of the maximum area problem intermediate between packing and covering, we have found that the generalized tensegrity structure model introduced in this paper is an effective tool. Here, at every circle arrangement, internal forces arise automatically in the associated tensegrity structure, but among them, that arrangement is optimal where the internal forces are in equilibrium. The complete (tangent) stiffness matrix of the tensegrity structures associated to the circle arrangements helped us to determine the exact values of the circle radius where the equilibrium paths bifurcate, that is, where the circle configurations change. Catastrophy theory provided additional insight into the stability properties of the circle arrangements. Hopefully, the tensegrity structure model presented here can be extended to analyse intermediate problems on the sphere as well.

Acknowledgement

Support by OTKA Grant No. K81146 is gratefully acknowledged.

References

[1] K. Bezdek, Über einige Kreisüberdeckungen. *Beitr. Alg. Geom.* **14**:7-13, 1983.
[2] P. Brass, W. Moser and J. Pach, *Research Problems in Discrete Geometry*, Springer, New York, 2005.
[3] R. Connelly, Maximizing the area of unions and intersections of discs. Lecture at the *Discrete and Convex Geometry Workshop*, Alfréd Rényi Institute of Mathematics, Budapest, July 4-6. 2008.
[4] B. Csikós, On the volume of the union of balls. *Discrete Computational Geometry* **20**(4):449-461, 1998.
[5] L. Fejes Tóth, *Regular Figures*, Pergamon, Macmillan, New York, 1964.
[6] P.W. Fowler and T. Tarnai, Transition from spherical circle packing to covering: geometrical analogues of chemical isomerization. *Proceedings of the Royal Society of London A* **452**:2043-2064, 1966.
[7] Zs. Gáspár, Mechanical models for the subclasses of catastrophes. In: M. Pignataro, V. Gioncu (eds): *Phenomenological and Mathematical Modelling of Structural Instabilities*. CISM Courses and Lectures No. 470, pp. 277-336, Springer, Wien, New York, 2005.
[8] R.L. Graham, Sets of points with given minimum separations (Solution to Problem E 1921). *Amer. Math. Monthly* **75**:192-193, 1968.
[9] T. Tarnai and Zs. Gáspár, Improved packing of equal circles on a sphere and rigidity of its graph. *Mathematical Proceedings of the Cambridge Philosophical Society* **93**:191-218, 1983.
[10] T. Tarnai and Zs. Gáspár, Covering the sphere by equal circles, and the rigidity of its graph. *Mathematical Proceedings of the Cambridge Philosophical Society* **110**:71-89, 1991.